Title

Differential bone adaptation to mechanical unloading and reloading in young, old, and osteocyte deficient mice

Authors

Cunningham, Hailey C
Orr, Sophie
Murugesh, Deepa K
et al.

Publication Date

2023-02-01

DOI

10.1016/j.bone.2022.116646

Peer reviewed

HHS Public Access

Author manuscript

Bone. Author manuscript; available in PMC 2023 April 06.

Published in final edited form as:

Bone. 2023 February ; 167: 116646. doi:10.1016/j.bone.2022.116646.

Differential Bone Adaptation to Mechanical Unloading and Reloading in Young, Old, and Osteocyte Deficient Mice

Hailey C. Cunningham[1], **Sophie Orr**[1], **Deepa K. Murugesh**[2], **Allison W. Hsia**[1], **Benjamin Osipov**[1], **Lauren Go**[3], **Po Hung Wu**[3], **Alice Wong**[4], **Gabriela G. Loots**[1,2], **Galateia J. Kazakia**[3], **Blaine A. Christiansen**[1]

[1]:University of California Davis Health, Department of Orthopaedic Surgery, 2700 Stockton Blvd, Suite 2301, Sacramento, CA 95817

[2]:Lawrence Livermore National Laboratory, 7000 East Avenue, L-452, Livermore, CA 94550

[3]:University of California San Francisco, Department of Radiology & Biomedical Imaging, 185 Berry Street, Bldg B, San Francisco, CA 94158

[4]:University of California Davis, School of Veterinary Medicine, 1285 Veterinary Medicine Dr, Bldg VM3A, Rm 4206, Davis, CA 95616

Abstract

Mechanical unloading causes rapid loss of bone structure and strength, which gradually recovers after resuming normal loading. However, it is not well established how this adaptation to unloading and reloading changes with age. Clinically, elderly patients are more prone to musculoskeletal injury and longer periods of bedrest, therefore it is important to understand how periods of disuse will affect overall skeletal health of aged subjects. Bone also undergoes an age-related decrease in osteocyte density, which may impair mechanoresponsiveness. In this study, we examined bone adaptation during unloading and subsequent reloading in mice. Specifically, we examined the differences in bone adaptation between young mice (3-month-old), old mice (18-month-old), and transgenic mice that exhibit diminished osteocyte density at a young age (3-month-old BCL-2 transgenic mice). Mice underwent 14 days of hindlimb unloading followed by up to 14 days of reloading. We analyzed trabecular and cortical bone structure in the femur, mechanical properties of the femoral cortical diaphysis, osteocyte density and cell death in cortical bone, and serum levels of inflammatory cytokines. We found that young mice lost ~10% cortical bone volume and 27-42% trabecular bone volume during unloading and early reloading, with modest recovery of metaphyseal trabecular bone and near total recovery of epiphyseal trabecular bone, but no recovery of cortical bone after 14 days of reloading. Old mice lost 12-14% cortical bone volume and 35-50% trabecular bone volume during unloading and early reloading but had diminished recovery of trabecular bone during reloading and no recovery of cortical bone. In BCL-2 transgenic mice, no cortical bone loss was observed during unloading or reloading, but 28-31% trabecular bone loss occurred during unloading and early reloading, with little to no recovery during reloading. No significant differences in circulating inflammatory cytokine

Corresponding Author: Blaine A. Christiansen, University of California Davis Health, Department of Orthopaedic Surgery, Lawrence J. Ellison Musculoskeletal Research Center, 2700 Stockton Blvd, Suite 2301, Sacramento, CA 95817, *Phone:* 916-734-3974, bchristiansen@ucdavis.edu.

levels were observed due to unloading and reloading in any of the experimental groups. These results illustrate important differences in bone adaptation in older and osteocyte deficient mice, suggesting a possible period of vulnerability in skeletal health in older subjects during and following a period of disuse that may affect skeletal health in elderly patients.

Keywords

Hindlimb unloading; osteocytes; aging; bone adaptation; cortical porosity

1. Introduction

Bone loses strength and structure with age [1–4], and old bone tissue is less mechanoresponsive to both increased and decreased loading [5, 6]. However, there is still only a limited understanding of specific age-related differences in bone's response to disuse and the mechanisms behind these differences. Elderly patients make up a disproportionately large number of hospitalizations, and their length of stay for hospitalizations is longer on average than younger adults [7, 8]. As a result, the reduced mechanical loading of bone during a hospitalization could have long-term consequences on the musculoskeletal health of elderly patients who are hospitalized for an extended amount of time. A more complete understanding of how bone adapts to decreased loading with age is therefore critical for protecting the skeletal health of elderly patients.

Osteocyte density in older people is ~30-40% lower than in younger patients in their 20s and 30s [9, 10]. Osteocytes are the major resident cells in bone tissue that sense changes in mechanical loading, therefore a decrease in osteocyte density could affect the bone tissue's ability to adapt to decreasing and increasing loads [11, 12]. Genetic mouse models can be used to investigate the effect of the age-related decrease in osteocyte density without other confounding factors associated with aging. One such genetic model is the BCL-2 transgenic mouse established and described by Moriishi *et al.* [13]. In this mouse model, human B-cell lymphoma 2 (BCL-2) is overexpressed in osteoblasts and osteocytes under the control of the Col1a1(2.3kb) promoter. Osteoblasts in this mouse model have suppressed cell adhesion, spreading, and mobility [13]. Osteocytes embedded in the bone matrix have fewer, shorter cell processes, and as a result the canalicular network is disrupted and the osteocytes are unable to obtain proper nutrition and eliminate waste, leading to cell death. By 10 weeks of age, approximately 50% of osteocytes are dead and by 16 weeks of age 75% of osteocytes have died [13, 14], establishing these mice as a model for studying the effects of osteocyte dysfunction. These mice exhibit increased trabecular and cortical bone volume in the tibia and femur compared to wild type mice, but do not exhibit any differences in bone volume in the spine at 4-weeks-old [13] and 4-months-old [14].

In this study, we investigated the differences in bone adaptation to unloading and subsequent reloading between young and old C57BL/6J mice, and in young BCL-2 transgenic mice as a model of osteocyte dysfunction. We hypothesized that old mice would have a decreased and delayed adaptation response to changes in the mechanical loading environment when compared with young mice due to diminished osteocyte signaling. We further hypothesized

that BCL-2 transgenic mice would have a decreased bone adaptation response to unloading and reloading compared to young wild-type mice but similar to the response of old mice. These findings would establish key differences and mechanisms of bone adaptation with age and decreased osteocyte density that may inform treatment strategies for elderly patients to maintain skeletal health during and after periods of disuse.

2. Materials and Methods

2.1 Animals

Male C57BL/6J and BCL-2 transgenic mice were used in these studies. Breeding pairs of BCL-2 Tg mice were provided to us by Dr. Toshihisa Komori, Nagasaki University, Nagasaki, Japan. C57BL/6J mice were purchased from the Jackson Laboratory (Sacramento, CA). All mice in this study belonged to one of three experimental groups: Young WT mice (n=47; 3-month-old C57BL/6J), Old WT mice (n=45; 18-month-old C57BL/6J), and BCL-2 transgenic mice (n=33; 3-month-old BCL-2 Tg). 3-month-old mice are analogous to 20-year-old people while 18-month-old mice are analogous to 56-year-old people [15]. Only male mice were used in this study, as we wanted to evaluate trabecular bone changes in the distal femoral metaphysis, and male mice retain considerably more trabecular bone in their hindlimbs at older ages compared to female mice [16]. Mice were cared for in accordance with the guidelines set by the National Institutes of Health (NIH) on the care and use of laboratory animals. All procedures were conducted under approved Institutional Animal Care and Use Committee protocols at UC Davis and Lawrence Livermore National Laboratory.

2.2 Experimental groups and study design

Mice were allowed to acclimate for 1-2 weeks in the vivarium prior to the start of the study. A subgroup of mice from each experimental group was euthanized at day 0 to establish baseline bone properties. All other mice underwent a period of tail suspension for up to 14 days as described below. One subgroup of mice from each experimental group was euthanized after 2 days of tail suspension while remaining mice underwent 14 days of tail suspension. Another subgroup of mice was euthanized immediately after the 14-day unloading period without resuming normal cage activity. Remaining mice were allowed to resume normal cage activity (reloading) for either 2 or 14 days after the unloading period. Subgroups of Young WT and Old WT mice included 8-10 mice per time point. Subgroups of BCL-2 Tg mice included 6-8 mice per time point. Experimental groups, terminal time points and group sizes are presented in Table 1.

At each terminal time point, mice were euthanized by exsanguination *via* cardiac puncture under anesthesia followed by cervical dislocation. Blood was collected during cardiac puncture for use in serum ELISA analysis described below and hindlimb bones were collected and stored as described below for micro-computed tomography analysis and histology.

2.3 Hindlimb unloading via tail suspension

Mice were subjected to hindlimb unloading *via* tail suspension as first described by Morey-Holten [17]. Mice were anesthetized with isoflurane, the tail was sterilized with an alcohol wipe, and a thin strip of skin-safe medical tape was wrapped around the base of the tail to minimize irritation. A U-shaped piece of wire was threaded through a swivel on an acrylic loop and attached to the base of the tail with cyanoacrylate. Once the wire hook was securely attached to the tail, the hook and tail were wrapped with additional skin-safe medical tape to reduce skin irritation and prevent mice from biting at the tail fixture. Mice were individually housed in custom-made cages with wire mesh flooring placed over absorbent pads; the acrylic loop at the top of the hook assembly was placed on a metal rod extending across the top of the cage. This assembly allowed the mice to move around their cage and access food, water, and nesting materials with their front limbs, but their hind limbs were unable to touch the floor of the cage (approximately 30-degree head-down angle).

2.4 Histology: TUNEL staining

Terminal deoxynucleotidyl transferase dUTP nick end labeling (TUNEL) staining was performed on histological sections of tibias from mice at baseline, after 14 days of unloading, and after 14 days of reloading to quantify differences in osteocyte density and osteocyte death between experimental groups (Young WT, Old WT and BCL-2 Tg). Following euthanasia, tibias were fixed in a 4% paraformaldehyde (PFA) solution for 5-7 days and then stored in 70% ethanol until decalcification. Tibias were decalcified with 0.5 M Ethylenediaminetetraacetic acid (EDTA) until fully decalcified as determined *via* x-ray. Decalcified tibias (n=2 per subgroup, n=18 total) were processed for paraffin embedding and 6 μm sagittal sections were cut from the mid diaphysis to proximal end of the tibia. Sections were stained for TUNEL using the Apoptag® system (Millipore Sigma, Temecula, CA). For each stained section, three areas of cortical bone were imaged at 20x magnification and analyzed for live and apoptotic osteocytes. Live osteocytes stained blue while TUNEL positive dead osteocytes stained brown. Sections were analyzed for relative differences in number of live osteocytes, dead osteocytes, and empty lacunae normalized to the surface area of the section analyzed.

2.5 Micro-computed tomography analysis of trabecular and cortical bone

Following euthanasia, left femurs were collected and preserved in 70% ethanol, then scanned *via* micro-computed tomography (SCANCO μCT 35, Brüttisellen, Switzerland) at X-ray tube potential 55 kVp, intensity 114 mA, integration time 900 ms, 6 μm isotropic nominal voxel size [18]. Trabecular bone analysis was performed at the distal metaphysis and distal epiphysis of the femur. Cortical bone analysis was performed at the mid diaphysis.

The epiphyseal region of interest began immediately proximal to the distal subchondral bone plate and included all trabecular bone between the subchondral bone plate and the distal growth plate. Because this section was fully enclosed by the growth plate, the size of region of interest for the epiphysis varied from sample to sample in the range of 70-110 slices or 0.42-0.66 mm in length. The metaphysis was defined as the trabecular bone within 200 slices (1.2 mm) of the region immediately proximal to the distal growth plate. A global threshold of 562.8 mg HA/cm^3 was used to segment “bone” from “non-bone” voxels for

all experimental groups. Trabecular bone parameters were calculated in both regions with the manufacturer's 3D analysis software and included: trabecular bone volume fraction (BV/TV), trabecular number (Tb.N), trabecular thickness (Tb.Th), and trabecular separation (Tb.Sp).

The region of interest for the cortical bone analysis was the mid-diaphysis, defined as a 200 slice (1.2 mm) region centered on 50% of the femur's total length. Bone area (B.Ar), total cross-sectional area (T.Ar), bone area fraction (B.Ar/T.Ar), cortical thickness (Ct.Th), and other parameters were calculated using the manufacturer's 3D analysis software. Additional parameters needed to calculate material properties from three-point bending mechanical testing data were obtained from μCT analysis, including the minimum moment of inertia (I_{min}) and the distance to the neutral axis (c).

Cortical bone porosity (i.e., pore volume fraction, PV/TV) was also analyzed at the mid-diaphysis and distal metaphysis at baseline, after 14 days of unloading, and after 14 days of reloading. Cortical bone was isolated from the trabecular compartment using semi-automated segmentation protocols in 3D Slicer (v 4.11.0, slicer.org). In brief, an initial cortical bone volume generated by thresholding the grayscale μCT images was manually corrected on 10 equally spaced slices. The final cortical bone volume was then generated by linearly interpolating between corrected slices and filling pore space using morphological processing. The cortical pore volume was generated by extracting void voxels inside the final cortical bone volume. Mid-diaphysis volumes were initially analyzed with PV/TV including large porosities ("macropores") that were present in BCL-2 Tg mice. A second analysis was also conducted that excluded these large porosities to determine their impact on overall cortical porosity.

2.6 Three-point bending mechanical testing

After μCT scanning, left femurs were mechanically tested in three-point bending to determine structural and material properties. Prior to testing, femurs were rehydrated by submerging them in a solution of phosphate buffeted saline for at least 10 minutes. Rehydrated femurs were then loaded into the mechanical testing machine (ELF 3200, TA Instruments, New Castle, DE) in a three-point bending setup such that the midpoint of the bone was directly beneath the top loading platen. The two lower platens were separated by 8 mm. To prevent motion or rotation of the bone during the test, the top actuator was lowered onto the sample to apply a small preload (typically 1-2 N). Samples were tested with the posterior aspect of the bone loaded in tension. Femurs were loaded to failure by a single monotonic load at a rate of 0.01 mm/sec. Force and displacement data were recorded at 50 Hz. Using the output force-displacement data, the linear region was isolated, and the yield point was identified as the point at which the force-displacement curve became non-linear. Stiffness of the linear region (K), yield force (F_Y), and ultimate force (F_{ult}) were determined from the force-displacement curve. Minimum moment of inertia (I_{min}) and the distance to the neutral axis (c) were used to calculate elastic modulus (E), yield stress, and ultimate stress using beam theory equations [19].

2.7 Serum cytokine analysis

Blood was spun at 1000g for 10 minutes at 4°C and the serum was stored at −80°C until analyzed. Enzyme-linked immunosorbent assay (ELISA) was used to measure circulating levels of Interleukin 6 (IL-6), Interleukin 1 beta (IL-1β) and tumor necrosis factor alpha (TNFα), in the isolated serum according to the manufacturer's instructions (Meso Scale Discovery, Rockville, MD).

2.8 Statistical analysis

Statistical analysis of μCT, mechanical testing, and ELISA data was performed *via* 2-way ANOVA with experimental group and time point as factors. Statistical significance was defined as $p < 0.05$. Main effects and interactions between experimental groups were obtained through the ANOVA. Since Old WT and BCL-2 Tg mice differed both in age and genotype, no direct statistical comparisons were made between these two groups. Instead, both of those experimental groups were compared only to Young WT mice.

To determine differences between subgroups (time points) within each experimental group, *post hoc* planned contrasts were performed. To adjust for the multiple comparisons from planned contrasts, the cutoff p-value for statistical significance was adjusted with a Bonferroni correction. The *p-value* (originally set at $p < 0.05$) was divided by the total number of contrasts which was 30. Thus, statistical significance in each planned contrast was defined as $p < 0.00167$.

3. Results

3.1 Histology: TUNEL staining

Histological assessment of TUNEL stained sections showed that at baseline, Old WT mice (Fig. 1b) had more extensive osteocyte death than Young WT mice (Fig. 1a). BCL-2 Tg mice (Fig. 1c) had greater overall lacunar density than either Young or Old WT mice (Fig. 1d), though the percentage of lacunae with live osteocytes was considerably lower in BCL-2 Tg mice than in Young WT mice. The total live osteocyte density in Old WT mice was lower than either Young WT or BCL-2 Tg mice (Fig. 1d). Empty lacunae (assumed to be dead osteocytes) were observed in samples from both Old WT mice and BCL-2 Tg mice, but no empty lacunae were observed in Young WT mice. After 14 days of unloading, live osteocyte density was lower in Young WT mice and BCL-2 Tg compared to baseline, but no decrease in osteocyte density was observed in Old WT mice (Fig. 1e). After 14 days of reloading, live osteocyte density had mostly recovered in Young WT mice and BCL-2 Tg mice. In contrast, live osteocyte density in Old WT mice was decreased at this time point relative to baseline.

3.2 Micro-Computed Tomography Analysis: Metaphyseal Trabecular Bone

At the metaphysis of Young WT mice, bone loss occurred during unloading and continued into early reloading, and only modest recovery was observed by 14 days of reloading (Fig. 2a–b). BV/TV and Tb.Th were significantly lower (−29% and −27%, respectively) than baseline after 14 days of unloading, and this bone loss was even greater (−42% and −34%, respectively) after 2 days of reloading. As expected, Old WT mice had less bone than Young WT mice at the metaphysis, but significant bone loss during unloading and reloading

was still observed in the Old WT mice. BV/TV in Old WT mice was 46% lower and Tb.Th was 36% lower after 14 days of unloading compared to baseline. These parameters remained lower than baseline for the full reloading period with little sign of recovery. In the metaphysis of BCL-2 Tg mice, no trabecular bone parameters were significantly different from baseline after 14 days of unloading. However, trabecular bone loss was observed throughout reloading at the metaphysis. After 14 days of reloading, both BV/TV and Tb.Th were significantly lower (−44% and −22% respectively) than baseline.

3.3 Micro-Computed Tomography Analysis: Epiphyseal Trabecular Bone

Similar patterns of trabecular bone loss and recovery were observed at the femoral epiphysis during unloading and reloading, though recovery during reloading was more complete at this site (Fig. 2c–d). In Young WT mice, BV/TV was 27% lower and Tb.Th was 23% lower at 14 days of unloading compared to baseline ($p < 0.0001$). During reloading, epiphyseal trabecular bone parameters in Young WT mice largely returned to baseline values after 14 days of reloading. Tb.Th returned to baseline values after 14 days of reloading, but BV/TV remained significantly lower than baseline at this time point (−12%, $p = 0.0013$). In Old WT mice, both BV/TV and Tb.Th were significantly lower (−35% and −26%, respectively) after 14 days of unloading compared to baseline ($p < 0.0001$). Following 14 days of reloading, epiphyseal BV/TV and Tb.Th significantly recovered but remained significantly lower than baseline. After 14 days of reloading, BV/TV remained 24% lower than baseline BV/TV ($p < 0.0001$) and Tb.Th remained 20% lower than baseline ($p < 0.0001$). In the epiphysis of BCL-2 Tg mice, we observed trabecular bone loss following unloading that did not recover during reloading. BV/TV was 28% lower and Tb.Th was 19% lower compared to baseline after 14 days of unloading ($p < 0.0001$). After 14 days of reloading, BV/TV and Tb.Th showed only non-significant trends toward recovery.

3.4 Micro-Computed Tomography Analysis: Mid-Diaphyseal Cortical Bone

Cortical bone microstructure did not change during unloading and reloading to the same extent as trabecular bone, but some bone loss was detected, particularly during reloading in Old WT mice (Fig. 3). In Young WT mice, after 14 days of reloading, Ct.Th was significantly lower (−11%) than the baseline value ($p = 0.0006$). Old WT mice also had significantly lower Ct.Th (−11%) after 14 days of unloading compared to baseline values ($p = 0.0005$) and remained lower (−17%) after 14 days of reloading ($p < 0.0001$). After 2 days of reloading, B.Ar of Old WT mice was significantly lower (−15.3%) than baseline ($p < 0.0001$). In contrast, no changes in cortical bone microstructure were observed at any time point in the BCL-2 Tg mice. Total cross-sectional area of Old WT mice was significantly greater than Young WT mice and BCL-2 Tg mice, consistent with periosteal expansion and endocortical resorption of bone during aging [20]. Total cross-sectional area of the femur did not change during unloading or reloading in any experimental group, indicating that changes in B.Ar and Ct.Th during unloading and reloading were attributable to endocortical bone resorption. Section modulus (a correlate of bending strength) was significantly decreased (−14%) after 2 days and 14 days of reloading in Old WT mice, but did not change during unloading or reloading in Young WT mice or BCL-2 Tg mice.

3.5 Micro-Computed Tomography Analysis: Cortical Porosity

Cortical porosity was primarily affected by unloading and reloading in BCL-2Tg mice (Fig. 4). PV/TV did not change after 14 days of unloading or 14 days of reloading in Old WT mice and was significantly decreased (−26%) in Young WT mice only after 14 days of reloading. In BCL-2 Tg mice, PV/TV was significantly increased after 14 days of reloading at the mid-diaphysis (+240%). However, this increase can be primarily attributed to expansion of the “macropores” in the cortical bone. Analysis of PV/TV in BCL-2 Tg mice excluding the macropores yielded results similar to those of Young WT mice, with a significant decrease in PV/TV (−32%) relative to baseline after 14 days of reloading. Similarly, at the distal femur no significant changes in PV/TV due to unloading or reloading were observed for Young or Old WT mice but decreases in PV/TV were observed in BCL-2 Tg mice after 14 days of unloading (−18% relative to baseline) and after 14 days of reloading (−48% relative to baseline).

3.6 Three-Point Bending Mechanical Testing

Three-point bending results largely mirrored the results from the cortical bone structure analysis (Fig. 5). We observed significant decreases in structural and material properties following unloading and reloading in Young and Old WT mice, but we observed no changes in bone mechanical properties following unloading or reloading in BCL-2 Tg mice. In Young WT mice, the elastic modulus was 25% lower after 2 days of unloading and remained significantly lower than baseline after 14 days of reloading; no other mechanical properties changed relative to baseline at any other time point. In contrast, unloading affected multiple mechanical properties in Old WT mice. After 14 days of unloading, femurs from Old WT mice had a significantly lower stiffness (−33%; $p = 0.0038$) and ultimate stress was significantly lower (−25%; $p = 0.0004$) than at baseline. After 14 days of reloading, the elastic modulus of femurs from Old WT mice was significantly lower than at baseline (−44%; $p < 0.0005$). No mechanical properties changed during unloading and reloading in BCL-2 Tg mice, but post-yield displacement was significantly lower in these mice relative to Young WT and Old WT mice. This is consistent with previous studies of mouse models of osteocyte deficiency, which showed that diminished osteocyte function resulted in bone tissue becoming more brittle [21].

3.7 Serum Cytokine Analysis

Serum cytokine measures had high variability within experimental groups, and thus we observed significant main effects between groups but no significant differences due to unloading or reloading (Supplemental Fig. 1). A significant main effect was observed between Young WT mice and Old WT mice, with Young WT mice having higher IL-1β and lower TNF-α than Old WT mice ($p < 0.0001$ and $p < 0.0001$, respectively). In addition, Young WT mice had higher IL-1β than BCL-2 Tg mice ($p < 0.0001$).

4. Discussion

In this study, we investigated differences in bone adaptation in response to unloading and reloading between three different experimental groups of mice: Young WT mice, Old WT mice, and BCL-2 Tg mice. Contrary to our initial hypothesis, Old WT mice had a robust

bone adaptation response to unloading that was similar in effect size to Young WT animals. Similarly, BCL-2 Tg mice, a model of osteocyte dysfunction, exhibited notable trabecular bone loss during unloading and reloading. However, we also observed key differences in bone adaptation between these experimental groups, particularly during reloading period, that may inform treatments and therapeutic targets for maintaining bone health during periods of disuse in older individuals.

The effect of disuse on bone in young adult subjects has been well established. In humans, bedrest and spaceflight studies have shown a gradual loss of bone mineral density (BMD) during periods of reduced loading. In bedrest studies, adult women exhibited a 3-4% decrease in trabecular BMD in the femur and tibia during a 60-day bedrest [22]. Though the scope of subjects was far narrower, spaceflight studies have indicated similar levels of trabecular bone resorption, with an estimated 1-2% loss of trabecular bone BMD in the hip per month spent in microgravity [23, 24]. In mouse tail suspension studies, 25-40% of trabecular bone volume fraction in the femur and tibia was lost over a 14-day period of unloading [25, 26]. Far fewer studies have examined the bone recovery that occurs during reloading following a period of unloading. Previous studies established that bone recovery during reloading takes far longer than the duration of unloading, up to twice as long as the unloading period [27–30]. Some studies indicate that even after full recovery of some bone quantity measures (i.e., BV/TV), the effects on other bone quality measures such as osteoblast number and bone formation rate may take even longer to recover [27, 29–32]. However, it is important to note that these reloading studies were done in adolescent or young adult populations. Therefore, these results may not necessarily translate to older subjects, and changes in bone metabolism with age could affect bone adaptation during unloading and subsequent reloading.

It has been reported that exercise in older patients results in smaller increases in bone mass than in younger patients [33]. Similarly, in animal models increased compression of cortical bone resulted in less bone formation in older animals than in younger animals [5]. However, far fewer studies have examined the effect of disuse on the bones of older people or animals. Previous studies in rats, including reports from our group, showed that the bones of older animals do not lose as much bone during unloading as younger animals [6, 34]. In addition, in our previously published work we observed that old rats continued to lose bone during reloading, which could imply that the adaptation response to decreased mechanical loading was delayed in older rats.

In this study we regularly observed bone loss during unloading that continued during the reloading period. There are a few potential causes for this continued bone loss during reloading. One potential explanation is that it may take a significant period of time after the end of unloading to reverse unloading-induced bone resorption. Trabecular bone loss during reloading occurred in early reloading with partial recovery later in reloading. In contrast, cortical bone loss continued during late reloading. This is reasonable, since trabecular bone is a more dynamically remodeled tissue than cortical bone and is quicker to respond to changing mechanical loading environments [27, 35]. Another potential cause for bone loss during reloading could be that allowing a mouse to ambulate with its hindlimbs after 14 days of unloading could cause microdamage to the bone from the sudden increase in mechanical

loading. The mechanostat theory suggests that if strain magnitude in bone is above a certain threshold, bone accrues damage rather than just adapting with a net increase in bone mass [36, 37]. It is possible that due to unloading-induced bone loss compromising the structure of the bone, there may be a period during early reloading where the strain magnitudes may be high enough to accrue some amount of damage, and this might be the initiating event for the bone loss that we observed in early reloading.

A previous study reported very little bone adaptation in old rats during unloading [6]. Similarly, in our previous study in rats, we observed no significant decreases in trabecular bone during 14 days of unloading, and we observed no significant decreases in cortical bone during unloading or subsequent reloading [34]. In contrast, in the current study we found that Old WT mice experienced considerable trabecular and cortical bone loss during unloading and reloading. It is somewhat difficult to compare our results, since previous studies examining unloading in older animals have used rats and have generally not reported epiphyseal bone results. Nonetheless, we did observe that Old WT mice did respond differently than Young WT mice during reloading. While both ages of WT mice experienced some continued bone loss during early reloading, Old WT mice did not exhibit the same magnitude of trabecular bone recovery. Similarly, BCL-2 Tg mice exhibited a clearly diminished ability to recover from bone loss during reloading, implicating osteocytes as a potential mediator of bone recovery during reloading.

Few studies have examined the effect of disuse on the bones of old animals, and these previous studies used ~28-month-old rats, whereas our study used 18-month-old mice. The rats in these previous studies were older relative to their total life span than the mice used in the current study, and this may explain some of the differences in bone adaptation that we observed in Old WT mice in this study versus previous studies in rats. Another factor that could contribute to the differences in the magnitude and timing of bone adaptation could be the differences in basal metabolic rate between mice and rats. Mice have a significantly higher metabolic rate than rats [38, 39], which could mean that the same 14-day period of mechanical unloading could have a much larger effect on the more metabolically active mouse than on the rat.

Young BCL-2 Tg mice were used in this study as a model of osteocyte dysfunction without the other confounding effects of aging. Since osteocytes have a key role in sensing and responding to mechanical loads in bone, osteocyte death and diminished lacunar-canalicular connectivity would suggest that BCL-2 Tg mice would have diminished bone adaptation in response to changing mechanical loading environments. A previous study showed that tail suspension in this BCL-2 Tg mouse model resulted in no significant trabecular bone loss in the metaphysis in response to unloading when the mice were 16 weeks old at the start of unloading [14]. In the current study, we similarly observed no significant loss of trabecular bone in the metaphysis during the unloading period. However, we did observe trabecular bone loss in the epiphysis during unloading, and we observed trabecular bone loss in the metaphysis when we investigated BCL-2 mice during reloading.

Previous studies have found that osteocyte apoptosis precedes disuse-induced bone loss [12, 40] and is localized to areas of microdamage in response to increased loading [41, 42].

While osteocyte apoptosis during reloading has not been directly measured, another study has modeled bone recovery during reloading using osteocyte viability based on the expected mechanical loading range that allows for osteocyte survival [43]. In the current study, we observed decreases in the number of live osteocytes following 14 days of unloading in all experimental groups. Unexpectedly, we also observed recovery of live osteocyte numbers after 14 days of reloading in Young WT and BCL-2 Tg mice. This observation certainly merits further investigation, and is difficult to explain since dead osteocytes are likely not replaced or reanimated during reloading. These observations may instead point to the difficulty in assessing live and dead osteocytes from paraffin-embedded sections. A previous study found that quantifying live/dead osteocytes from paraffin sections overestimates the numbers of empty lacunae due to shrinkage of osteocytes during processing, and that assessment of osteocytes using plastic sections is more accurate [20].

BCL-2 Tg mice had a considerably higher density of osteocyte lacunae than C57BL/6J mice. This may be due to the fact that BCL-2 is known to block cell apoptosis, so potentially a higher number of osteoblasts survived to become osteocytes before ultimately dying due to the disrupted lacunar-canalicular network. A lower number of live osteocytes at baseline means that there are fewer osteocytes that can undergo cell death in response to either unloading or reloading, which may impair bone adaptation. Cortical bone microstructure in BCL-2 Tg mice did not change during unloading or reloading (though there were notable changes in cortical porosity), and there were no differences observed in mechanical properties at any time point. Mechanoresponsiveness, particularly in the diaphysis of long bones, is thought to be heavily mediated by osteocytes [11, 44] and thus a lower osteocyte density and dysfunctional canalicular network in the BCL-2 Tg mice could explain the lack of cortical bone response to unloading and reloading in these mice. Furthermore, the development of “macropores” in BCL-2 Tg mice suggests that osteocyte dysfunction or death may contribute to trabecularization of cortical bone with age, though specific mechanisms are not yet understood, and we did not investigate the content of cortical macropores in this study. Further research into these changes is warranted as increased porosity and trabecularization of cortical bone present a major risk for degradation of structural properties of bone and increased fracture risk in older subjects.

One limitation of this study is the cross-sectional design with multiple terminal time points; there are no analyses that captured the changes for the same animals over the course of the unloading and reloading periods. Additionally, this study used only male mice due to the paucity of trabecular bone in the metaphysis of older female C57BL/6J mice, therefore we were unable to assess potential differences in bone adaptation in male vs. female mice. We also purchased C57BL/6J mice from a vendor rather than using transgene-negative littermate controls to compare WT and BCL-2 Tg mice. In addition, this study is limited in the conclusions it can draw mechanistically. Our analysis presents a thorough examination of structural and mechanical changes in response to loading and unloading, but mechanistically we only examined TUNEL staining of osteocytes and serum levels of inflammatory cytokines. Thus, while we have observed complex differences in site-specific bone adaptation between the three experimental groups, we cannot currently determine the specific biological mechanisms causing these changes.

5. Conclusions

This study builds on our previous work examining age-related differences in bone adaptation during mechanical unloading and subsequent reloading. Here we describe a delay in bone recovery and additional bone loss during reloading in Old WT and BCL-2 Tg mice, which further indicates that there may be a window of skeletal vulnerability in older subjects following a period of disuse. Altered bone adaptation in BCL-2 Tg mice, particularly in cortical bone, provides further evidence of the role of osteocytes during bone's response to changing mechanical loading environments. This research motivates further investigations into specific differences in bone adaptation based on age and other factors to better preserve the skeletal health of elderly patients following significant periods of bedrest or disuse.

Supplementary Material

Refer to Web version on PubMed Central for supplementary material.

Acknowledgements:

We would like to thank Dr. Toshihisa Komori for generously sharing the BCL-2 transgenic mice with us. Dr. Christiansen is supported by the National Institute of Arthritis and Musculoskeletal and Skin Diseases under Award Numbers R01 AR071459 and R01 AR075013, and by the Department of Defense under Award Number PR180268P1. Dr. Kazakia is supported by the National Institute of Arthritis and Musculoskeletal and Skin Diseases under Award Numbers P30 AR075055 and R01 AR076159. Dr. Loots is supported by the Department of Defense under Award Number PR180268. The content is solely the responsibility of the authors; the funding bodies were not involved with the writing of this chapter. DKM and GGL performed work under the auspices of the U.S. Department of Energy by Lawrence Livermore National Laboratory under Contract DE-AC52-07NA27344. The authors have no conflicts of interest to disclose.

References

1. Goltzman D, The Aging Skeleton, in Human Cell Transformation: Advances in Cell Models for the Study of Cancer and Aging, Rhim JS, Dritschilo A, and Kremer R, Editors. 2019, Springer, Cham.
2. Burr DB, Muscle strength, bone mass, and age-related bone loss. J Bone Miner Res, 1997. 12(10): p. 1547–51. [PubMed: 9333114]
3. Burstein AH, Reilly DT, and Martens M, Aging of bone tissue: mechanical properties. J Bone Joint Surg Am, 1976. 58(1): p. 82–6. [PubMed: 1249116]
4. Gibon E, Lu L, and Goodman SB, Aging, inflammation, stem cells, and bone healing. Stem Cell Res Ther, 2016. 7: p. 44. [PubMed: 27006071]
5. Rubin CT, Bain SD, and McLeod KJ, Suppression of the osteogenic response in the aging skeleton. Calcif Tissue Int, 1992. 50(4): p. 306–13. [PubMed: 1571841]
6. Perrien DS, Akel NS, Dupont-Versteegden EE, Skinner RA, Siegel ER, Suva LJ, et al. Aging alters the skeletal response to disuse in the rat. Am J Physiol Regul Integr Comp Physiol, 2007. 292(2): p. R988–96. [PubMed: 17068163]
7. Czaja CA, Miller L, Alden N, Wald HL, Cummings CN, Rolfes MA, et al. Age-Related Differences in Hospitalization Rates, Clinical Presentation, and Outcomes Among Older Adults Hospitalized With Influenza-U.S. Influenza Hospitalization Surveillance Network (FluSurv-NET). Open Forum Infect Dis, 2019. 6(7).
8. Russo CA and Elixhauser A, Hospitalizations in the Elderly Population, 2003, in Healthcare Cost and Utilization Project (HCUP) Statistical Briefs. 2006: Rockville (MD).
9. Mullender MG, van der Meer DD, Huiskes R, and Lips P, Osteocyte density changes in aging and osteoporosis. Bone, 1996. 18(2): p. 109–13. [PubMed: 8833204]

10. Vashishth D, Verborgt O, Divine G, Schaffler MB, and Fyhrie DP, Decline in osteocyte lacunar density in human cortical bone is associated with accumulation of microcracks with age. Bone, 2000. 26(4): p. 375–80. [PubMed: 10719281]
11. Aarden EM, Burger EH, and Nijweide PJ, Function of osteocytes in bone. J Cell Biochem, 1994. 55(3): p. 287–99. [PubMed: 7962159]
12. Aguirre JI, Plotkin LI, Stewart SA, Weinstein RS, Parfitt AM, Manolagas SC, et al. Osteocyte apoptosis is induced by weightlessness in mice and precedes osteoclast recruitment and bone loss. J Bone Miner Res, 2006. 21(4): p. 605–15. [PubMed: 16598381]
13. Moriishi T, Maruyama Z, Fukuyama R, Ito M, Miyazaki T, Kitaura H, et al. Overexpression of Bcl2 in osteoblasts inhibits osteoblast differentiation and induces osteocyte apoptosis. PLoS One, 2011. 6(11): p. e27487. [PubMed: 22114675]
14. Moriishi T, Fukuyama R, Ito M, Miyazaki T, Maeno T, Kawai Y, et al. Osteocyte network; a negative regulatory system for bone mass augmented by the induction of Rankl in osteoblasts and Sost in osteocytes at unloading. PLoS One, 2012. 7(6): p. e40143. [PubMed: 22768243]
15. Flurkey K, Currer JM, and Harrison DE, Mouse models in aging research, in The mouse in biomedical research, Fox JG, et al. Editors. 2007, Elsevier: New York. p. 637–72.
16. Glatt V, Canalis E, Stadmeyer L, and Bouxsein ML, Age-related changes in trabecular architecture differ in female and male C57BL/6J mice. J Bone Miner Res, 2007. 22(8): p. 1197–207. [PubMed: 17488199]
17. Morey-Holton ER and Globus RK, Hindlimb unloading of growing rats: a model for predicting skeletal changes during space flight. Bone, 1998. 22(5 Suppl): p. 83S–88S. [PubMed: 9600759]
18. Bouxsein ML, Boyd SK, Christiansen BA, Guldberg RE, Jepsen KJ, and Muller R, Guidelines for assessment of bone microstructure in rodents using micro-computed tomography. J Bone Miner Res, 2010. 25(7): p. 1468–86. [PubMed: 20533309]
19. Jepsen KJ, Silva MJ, Vashishth D, Guo XE, and van der Meulen MC, Establishing biomechanical mechanisms in mouse models: practical guidelines for systematically evaluating phenotypic changes in the diaphyses of long bones. J Bone Miner Res, 2015. 30(6): p. 951–66. [PubMed: 25917136]
20. Tiede-Lewis LM, Xie Y, Hulbert MA, Campos R, Dallas MR, Dusevich V, et al. Degeneration of the osteocyte network in the C57BL/6 mouse model of aging. Aging (Albany NY), 2017. 9(10): p. 2190–2208. [PubMed: 29074822]
21. Vrahnas C, Blank M, Dite TA, Tatarczuch L, Ansari N, Crimeen-Irwin B, et al. Increased autophagy in EphrinB2-deficient osteocytes is associated with elevated secondary mineralization and brittle bone. Nat Commun, 2019. 10(1): p. 3436. [PubMed: 31366886]
22. Beller G, Belavy DL, Sun L, Armbrecht G, Alexandre C, and Felsenberg D, WISE-2005: bed-rest induced changes in bone mineral density in women during 60 days simulated microgravity. Bone, 2011. 49(4): p. 858–66. [PubMed: 21723970]
23. LeBlanc A, Schneider V, Shackelford L, West S, Oganov V, Bakulin A, et al. Bone mineral and lean tissue loss after long duration space flight. J Musculoskelet Neuronal Interact, 2000. 1(2): p. 157–60. [PubMed: 15758512]
24. Collet P, Uebelhart D, Vico L, Moro L, Hartmann D, Roth M, et al. Effects of 1- and 6-month spaceflight on bone mass and biochemistry in two humans. Bone, 1997. 20(6): p. 547–51. [PubMed: 9177869]
25. Cabahug-Zuckerman P, Frikha-Benayed D, Majeska RJ, Tuthill A, Yakar S, Judex S, et al. Osteocyte Apoptosis Caused by Hindlimb Unloading is Required to Trigger Osteocyte RANKL Production and Subsequent Resorption of Cortical and Trabecular Bone in Mice Femurs. J Bone Miner Res, 2016. 31(7): p. 1356–65. [PubMed: 26852281]
26. Sakai A and Nakamura T, Changes in trabecular bone turnover and bone marrow cell development in tail-suspended mice. J Musculoskelet Neuronal Interact, 2001. 1(4): p. 387–92. [PubMed: 15758489]
27. Basso N, Jia Y, Bellows CG, and Heersche JN, The effect of reloading on bone volume, osteoblast number, and osteoprogenitor characteristics: studies in hind limb unloaded rats. Bone, 2005. 37(3): p. 370–8. [PubMed: 16005699]

28. Shirazi-Fard Y, Anthony RA, Kwaczala AT, Judex S, Bloomfield SA, and Hogan HA, Previous exposure to simulated microgravity does not exacerbate bone loss during subsequent exposure in the proximal tibia of adult rats. Bone, 2013. 56(2): p. 461–73. [PubMed: 23871849]
29. Shirazi-Fard Y, Kupke JS, Bloomfield SA, and Hogan HA, Discordant recovery of bone mass and mechanical properties during prolonged recovery from disuse. Bone, 2013. 52(1): p. 433–43. [PubMed: 23017660]
30. Shirazi-Fard Y, Metzger CE, Kwaczala AT, Judex S, Bloomfield SA, and Hogan HA, Moderate intensity resistive exercise improves metaphyseal cancellous bone recovery following an initial disuse period, but does not mitigate decrements during a subsequent disuse period in adult rats. Bone, 2014. 66: p. 296–305. [PubMed: 24929241]
31. Lang TF, Leblanc AD, Evans HJ, and Lu Y, Adaptation of the proximal femur to skeletal reloading after long-duration spaceflight. J Bone Miner Res, 2006. 21(8): p. 1224–30. [PubMed: 16869720]
32. Keyak JH, Koyama AK, LeBlanc A, Lu Y, and Lang TF, Reduction in proximal femoral strength due to long-duration spaceflight. Bone, 2009. 44(3): p. 449–53. [PubMed: 19100348]
33. Daley MJ and Spinks WL, Exercise, mobility and aging. Sports Med, 2000. 29(1): p. 1–12. [PubMed: 10688279]
34. Cunningham HC, West DWD, Baehr LM, Tarke FD, Baar K, Bodine SC, et al. Age-dependent bone loss and recovery during hindlimb unloading and subsequent reloading in rats. BMC Musculoskelet Disord, 2018. 19(1): p. 223. [PubMed: 30021585]
35. Weatherholt AM, Fuchs RK, and Warden SJ, Cortical and trabecular bone adaptation to incremental load magnitudes using the mouse tibial axial compression loading model. Bone, 2013. 52(1): p. 372–9. [PubMed: 23111313]
36. Frost HM, The Utah paradigm of skeletal physiology: an overview of its insights for bone, cartilage and collagenous tissue organs. J Bone Miner Metab, 2000. 18(6): p. 305–16. [PubMed: 11052462]
37. Cowin SC, Wolff's law of trabecular architecture at remodeling equilibrium. J Biomech Eng, 1986. 108(1): p. 83–8. [PubMed: 3959556]
38. Terpstra AH, Differences between humans and mice in efficacy of the body fat lowering effect of conjugated linoleic acid: role of metabolic rate. J Nutr, 2001. 131(7): p. 2067–8. [PubMed: 11435531]
39. Agoston DV, How to Translate Time? The Temporal Aspect of Human and Rodent Biology. Front Neurol, 2017. 8: p. 92. [PubMed: 28367138]
40. Kennedy OD, Laudier DM, Majeska RJ, Sun HB, and Schaffler MB, Osteocyte apoptosis is required for production of osteoclastogenic signals following bone fatigue in vivo. Bone, 2014. 64: p. 132–7. [PubMed: 24709687]
41. Schaffler MB and Kennedy OD, Osteocyte signaling in bone. Curr Osteoporos Rep, 2012. 10(2): p. 118–25. [PubMed: 22552701]
42. Verborgt O, Gibson GJ, and Schaffler MB, Loss of osteocyte integrity in association with microdamage and bone remodeling after fatigue in vivo. J Bone Miner Res, 2000. 15(1): p. 60–7. [PubMed: 10646115]
43. Wang H, Ji B, Liu XS, van Oers RF, Guo XE, Huang Y, et al. Osteocyte-viability-based simulations of trabecular bone loss and recovery in disuse and reloading. Biomech Model Mechanobiol, 2014. 13(1): p. 153–66. [PubMed: 23584331]
44. Piekarski K and Munro M, Transport mechanism operating between blood supply and osteocytes in long bones. Nature, 1977. 269(5623): p. 80–2. [PubMed: 895891]

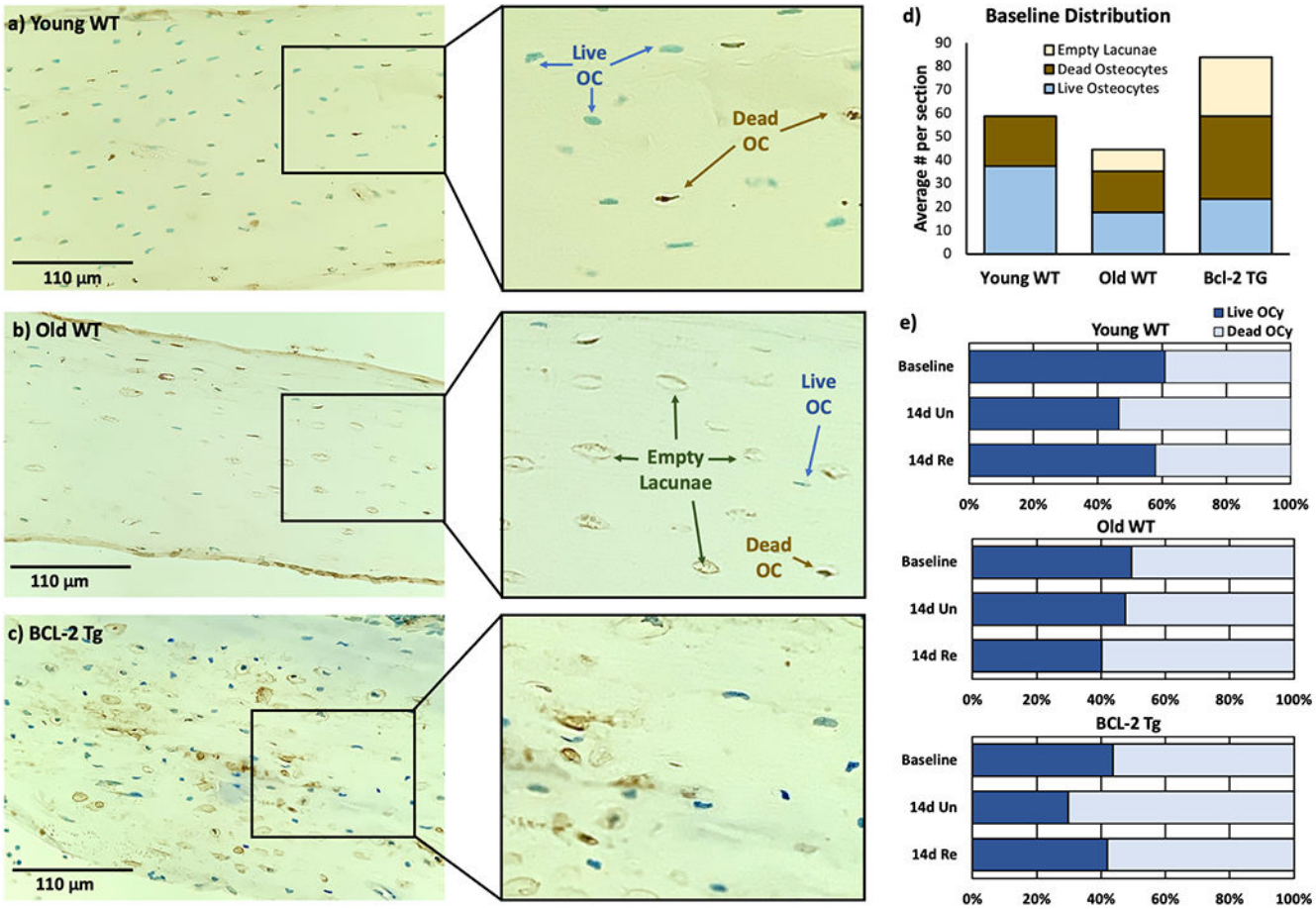

Figure 1:

(a-b) Representative images of TUNEL-stained osteocytes in tibias from Young WT (a), Old WT (b), and BCL-2 Tg (c) mice. Live osteocytes appear blue and dead osteocytes appear brown. Empty lacunae were also observed in Old WT mice and BCL-2 Tg mice. Old WT mice had a lower lacunar density overall compared to Young WT mice, with a greater percentage of dead osteocytes and empty lacunae (d). BCL-2 Tg mice had a higher lacunar density than Young WT mice, but a much lower percentage of live osteocytes (d). After 14 days of unloading, both Young WT mice and BCL-2 Tg mice had diminished live osteocyte density, but this seemed to recover after 14 days of reloading (e). In contrast, Old WT mice did not have a decrease in live osteocyte density after 14 days of unloading, but did exhibit decreased live osteocyte density after 14 days of reloading.

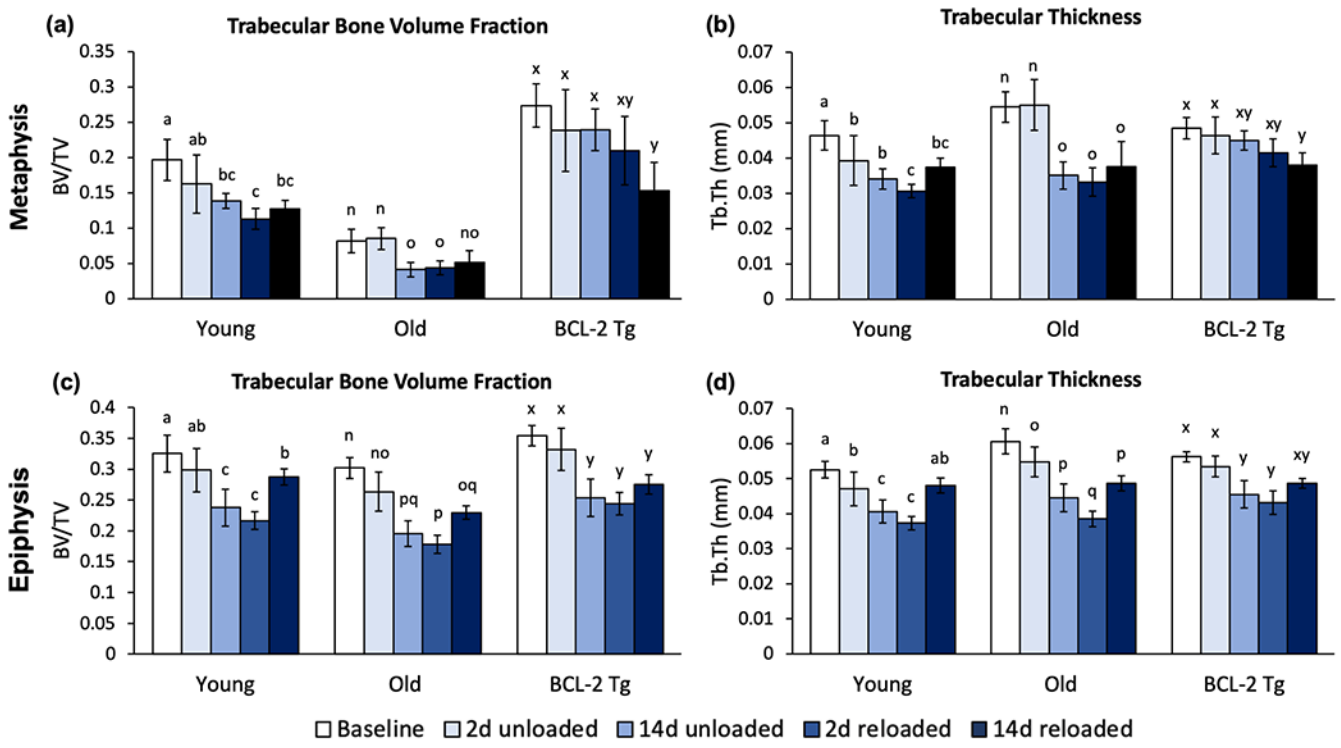

Figure 2:

Trabecular bone microstructure at the distal femoral metaphysis (a-b) and epiphysis (c-d). At the metaphysis, significant bone loss was observed in Young WT and Old WT mice after 14 days of unloading and into reloading, with little recovery after 14 days of reloading. In BCL-2 TG mice, bone loss was not observed after unloading, but significant bone loss occurred after 14 days of reloading. At the epiphysis, mice in all experimental groups had diminished bone volume and trabecular thickness after 14 days of unloading and into early reloading. This was largely recovered in Young WT and Old WT mice, but little recovery was observed in BCL-2 Tg mice. Data are presented as mean with standard deviation. On each graph, groups that do not share a letter are significantly different.

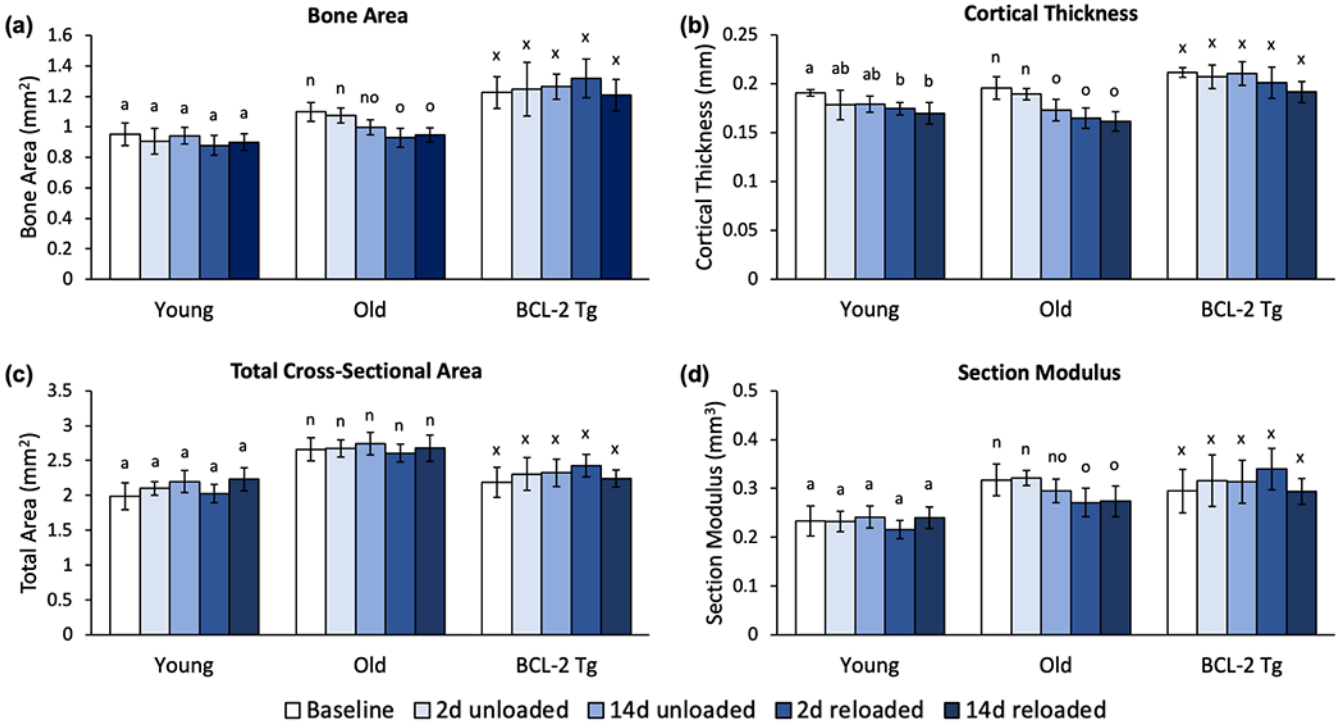

Figure 3:

Cortical bone microstructure at the femoral mid-diaphysis. Significant decrease in cortical thickness were observed in Old WT mice after 14 days of unloading, and this bone loss was maintained during reloading. In contrast, Young WT mice lost cortical thickness only after 2 or 14 days of reloading, and no cortical bone loss was observed in BCL-2 Tg mice. Bone area and section modulus were diminished in Old WT mice after 2 and 14 days of reloading, but these were not affected by unloading or reloading in Young WT or BCL-2 Tg mice.

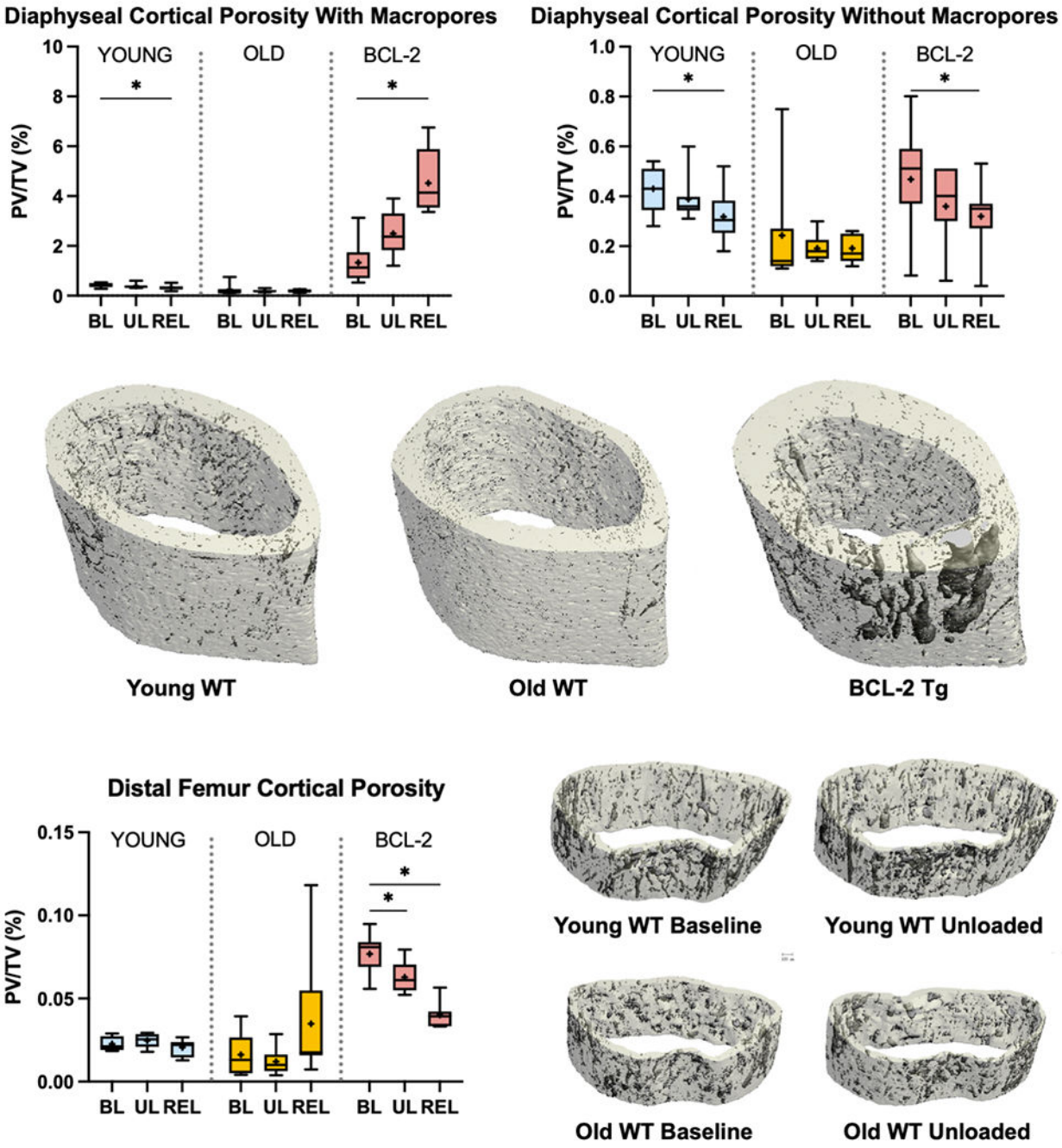

Figure 4:

Cortical porosity at the mid-diaphysis (top) and distal metaphysis (bottom). At the mid-diaphysis, BCL-2 Tg mice had considerably higher porosity than Young or Old WT mice, and this porosity was increased by unloading and reloading. When “macropores” were excluded from the analysis of BCL-2 Tg mice, Young WT mice and BCL-2 Tg mice had comparable cortical porosity, and both were significantly reduced during unloading and reloading. At the distal metaphysis, BCL-2 Tg mice had higher cortical porosity than either

Young or Old WT mice, and this porosity was reduced during unloading and reloading. No changes were observed as a result of unloading or reloading in Young or Old WT mice.

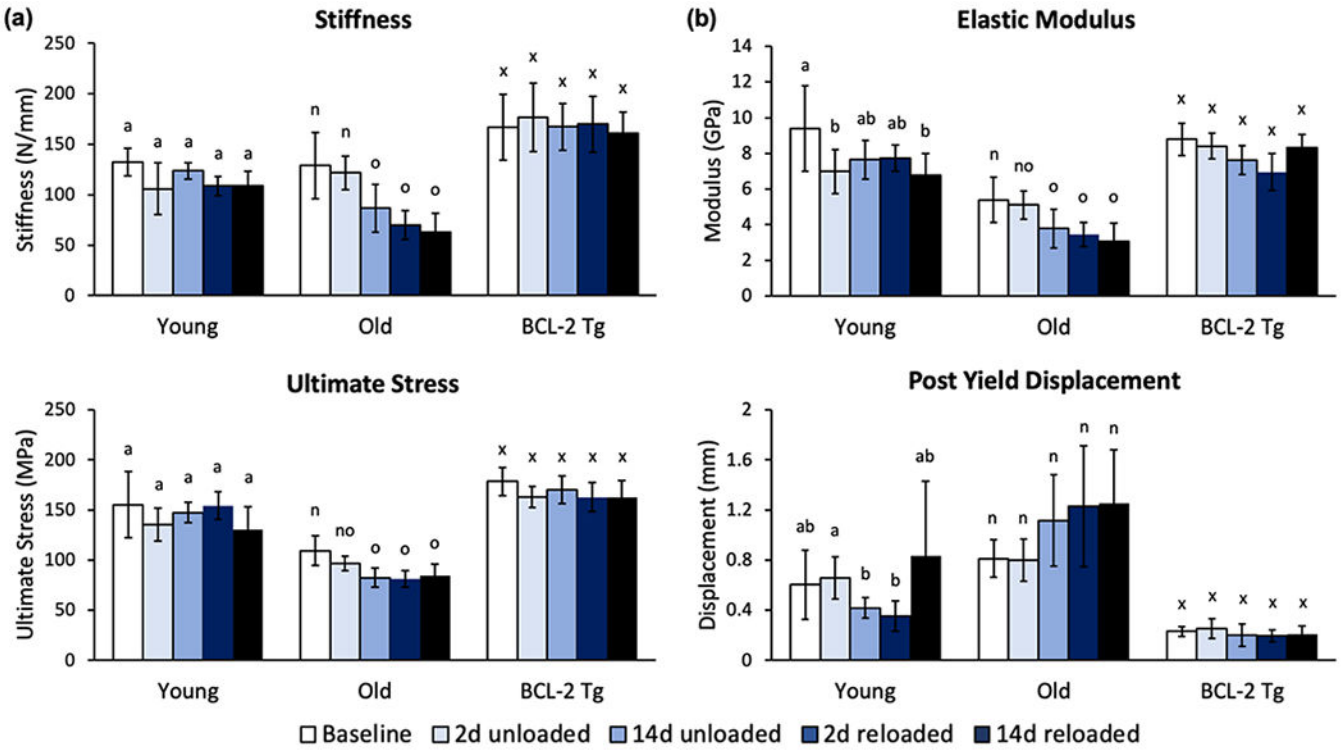

Figure 5:

Structural and material properties of femoral cortical bone determined by 3-point bending. Changes in structural and material properties of cortical bone largely mirrored microstructural changes in cortical bone, with the greatest effect of unloading observed in the Old WT mice, and little or no effect in Young WT and BCL-2 Tg mice. Data are presented as mean with standard deviation. On each graph, groups that do not share a letter are significantly different.

Table 1:

Experimental groups, terminal time points for subgroups, and subgroup sizes

Experimental Group	Baseline (Day 0)	2 days of unloading (Day 2)	14 days of unloading (Day 14)	2 days of reloading (Day 16)	14 days of reloading (Day 28)
Young WT (3 months old)	n=9	n=10	n=8	n=10	n=10
Old WT (18 months old)	n=8	n=10	n=10	n=9	n=8
BCL-2 Tg (3 months old)	n=6	n=8	n=6	n=6	n=7